

Surface and Subsurface Characteristics of NiCrBSi Coating with Different WC Amount Prepared by Flame Spray Method

Tharanon Usana-ampaipong¹ · Chaiya Dumkum¹ · Karuna Tuchinda² · Viboon Tangwarodomnukun¹  · Boonyawat Teeraprawatekul³ · Huan Qi⁴

Submitted: 17 September 2018 / in revised form: 16 January 2019 / Published online: 29 January 2019
© ASM International 2019

Abstract This research aims at understanding the spray coating of NiCrBSi with different amount of tungsten carbide particles on JIS SUP9 steel substrate. The amount of tungsten carbide added to NiCrBSi was 0, 20, and 40% by volume to reinforce the coating. Microstructures, microhardness, adhesion, cohesion, and rigidity of coating were characterized. The results revealed that NiCrBSi structure composed of nickel solid solution as matrix embedded with Ni boride and Ni₄Si with chromium carbide distributed across the coating. Tungsten carbide particles were apparent in the coating and they partially diffused into the NiCrBSi coating. In the case of 40% tungsten carbide addition, the matrix hardness was increased by 29.18%, but the cohesion of coating was reduced by 22.94%. The adhesion failure was not apparent in all samples examined in this study under the 20 N scratch load. Wear area of coatings mixed with tungsten carbide addition was found to decrease by 3.5 to 8.8 times compared to the substrate. As per the findings, the addition of WC can promote the wear resistance by its reinforcement and also introduce the solid

solution strengthening of W in the NiCrBSi matrix, specifically in the Ni solid solution.

Keywords NiCrBSi coating · solid solution strengthening · thermal spray coating · tungsten carbide

Introduction

Thermal spray process is a method to apply coating materials on a substrate for enhancing some surface properties (Ref 1, 2), e.g., bettering wear resistance, or for specific repairing purposes. The coating materials are melted by using heat from a combustion or electric arc. The molten elements are sprayed to the substrate surface where the molten droplets impact, splat and then solidify as a solid coating layer. This method is well known for its simplicity and inexpensive compared to other coating processes. However, its major drawbacks are splat morphology, oxide inclusion, and porosity, and these consequently result in delamination failure. Post-treatment process is generally applied to remedy these problems. Torch, induction, or furnace can be used for fusing the coating to additionally densify it (Ref 3). The subsequent fusion is commonly applied only for self-fluxing alloy or self-fluxing alloy-based coatings. Organic sealing can be applied to fill up the porosity in order to prevent any contaminant penetrating inside the coating (Ref 4).

NiCrBSi coating is one of the materials commonly applied in the thermal spray processes since it has good wear and corrosion resistances. Ni matrix offers good ductility and corrosion resistance, and Cr further enhances the wear resistance. B and Si suppress the melting temperature of coating material via eutectic reaction (Ref 5), thereby forming hard precipitate as a result. The NiCrBSi

✉ Viboon Tangwarodomnukun
viboon.tan@kmutt.ac.th

¹ Department of Production Engineering, Faculty of Engineering, King Mongkut's University of Technology Thonburi, Bangkok 10140, Thailand
² Department of Mechanical Engineering (Simulation and Design), The Sirindhorn International Thai-German Graduate School of Engineering, Bangkok 10800, Thailand
³ Acme International (Thailand) Ltd., Bangkok, Thailand
⁴ Key Laboratory of Special Purpose Equipment and Advanced Processing Technology, Ministry of Education & Zhejiang Province, Zhejiang University of Technology, Hangzhou 310014, China

coating is therefore suitable for most of surfacing processes, e.g., flame spray (Ref 3, 6), high velocity oxy-fuel combustion (HVOF) (Ref 3), atmospheric plasma spray (APS) (Ref 7-11), plasma transferred arc (PTA) (Ref 12), and laser cladding (LC) processes (Ref 6, 13-16), and each of which yields different microstructures (Ref 6). When high wear resistance of the coating is required, WC particles can be added to reinforce the NiCrBSi matrix. Due to the high hardness and high melting temperature of WC, it can be applied to the coating applications that wear is of great concern.

By considering high thermal energy processes such as welding, WC usually being in the form of W₂C or WC eutectic mixture is likely suffered from W₂C decarburization or dissolution, causing brittle phases, e.g., Ni₂W₄C (Ref 13), NiW, or NiCrW (Ref 10) and graphite precipitation under a certain high heat energy condition (Ref 10). This can in turn deteriorate coating hardness in macro-level to nano-level and wear resistance (Ref 13, 15, 17, 18). Monocrystalline WC is instead preferred for such high energy conditions, but it is costly and also induces lower hardness than eutectic variant (Ref 13, 17). Since a great amount of coating materials are melted in the process, there is a high plausibility for WC to sink at the bottom of coating layer or gather on the substrate surface due to the high density of WC (Ref 13, 14). This characteristic typically found in the welding processes, causing very little benefit of WC to reinforce the coating layer (Ref 14). Even in the atmospheric plasma spray process, W-rich solid solution (α_2) can also precipitate from NiCrW during its cooling (Ref 10).

Though the roles of WC in advancing the coating layer already noted in a number of studies, the effects of WC dissolution in NiCrBSi coating induced by the thermal spray process have not been comprehensively reported. This study therefore aims at investigating the influence of WC dissolution in the flame-sprayed NiCrBSi coating on a JIS SUP9 spring steel substrate. Microstructure, microhardness, adhesion, cohesion, and rigidity of coatings were observed and discussed to enable a further insight into the interactions between WC and NiCrBSi matrix in the thermal spray and fused process.

Experiment

Material

A substrate material was JIS SUP9 steel cut in the size of 20 × 20 × 5 mm before being blasted by alumina grit. Pre-alloyed gas atomized NiCrBSi powder (HMSP 1040-00, Höganäs AB, Sweden), and the fused and crushed mixture of WC and W₂C eutectic phase powder (HMSP 4070 WC, Höganäs AB, Sweden) were used as coatings materials in this study. The composition of JIS SUP9 steel and powders is shown in Tables 1 and 2, respectively. To realize the effects of WC on coating characteristics obtained, the WC powder of 0, 20, and 40% by volume was mixed with the NiCrBSi powder and then, all together was applied in the thermal spray process. The mixture was dried at 80 °C for an hour and then mixed by rotary mixer for 10 min before spraying.

Spraying Process

Flame spray was used as a deposition technique to create a coating layer in this work. The process was done at Acme International (Thailand) Ltd. using Duraloy series torch from Ibeda (Germany). The pressures of acetylene and oxygen used as a combustion fuel were set at 0.5 and 7 bar, respectively, and the consumption rate of each gas is 160 l/h. Spraying distance was kept constant at 30 mm, and the final coating thickness was kept at 0.5-0.6 mm for all tests in this study.

At the beginning of spraying process, a substrate was preheated by spray torch until its temperature of about 80 °C to prevent residue moisture in the substrate surface.

Table 2 Chemical composition NiCrBSi and WC powder

Materials	Size, μm	Chemical composition, wt.%						
		C	Si	B	Fe	Cr	Ni	W
NiCrBSi	20-106	0.25	3.5	1.6	2.5	7.5	Bal	...
WC	20-106	4	Bal

Table 1 Chemical composition of JIS SUP9 steel

Materials	Chemical composition, wt.%						
	C	Si	Mn	P	S	Cr	Fe
JIS SUP9	0.52-0.60	0.15-0.35	0.65-0.95	0.035 max	0.035 max	0.65-0.95	Bal

Then, the coating was applied over the substrate surface instantly to prevent surface oxidation. During the torch heating of work surface, the surface glowed shiny red, indicating the melting of coating materials. Spraying and in situ fusing of coating materials were then performed simultaneously. Once the spraying was completed, the substrate was cooled down inside vermiculite to slow the cooling rate and prevent cracking induced by thermal stress until the room temperature was reached.

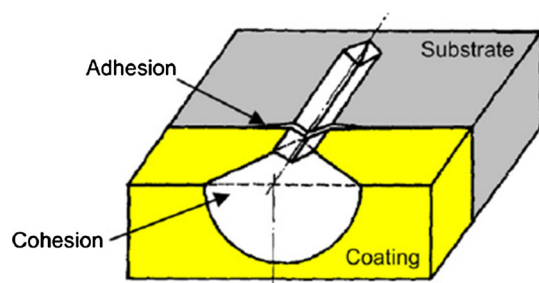


Fig. 1 Measurement of adhesion and cohesion associated with the scratch test method (Ref 9)

Characterization

Each sample was cut by a low-speed diamond saw, cold mounted by epoxy resin, grinded with 240, 400, 600, 800, 1000, and 1200 mesh SiC sandpapers, and subsequently polished by 1 and 0.3 μm Al_2O_3 slurry on a nap cloth. The polished samples were etched by a mixture of acetic, nitric, and hydrochloric acid with the ratio of 1:1:1, respectively, for 5 min. After the etching, the samples were rinsed in ethanol, dried and kept with silica gel to prevent any possible residual moisture.

Microstructures were observed by using a scanning electron microscope (JEOL JSM-6610 LV) and inspected the chemical composition by using energy dispersive spectroscopy (Oxford INCA 3350). Microhardness was quantified by Vickers microhardness tester using 0.1 kg load and 15 s dwell time. The indentation was done on the cross section of work samples, starting from the top of coating down to the substrate with 100- μm spacing. The hardness measurement was stopped at 200 μm below the substrate surface.

Cohesion and adhesion of NiCrBSi coating were characterized by using a scratch test technique (Ref 9). CSM Revetest Macro Scratch Tester equipped with a diamond indenter of 200- μm tip radius was employed to apply a constant load of 20 N and scratching speed of 0.33 mm/s.

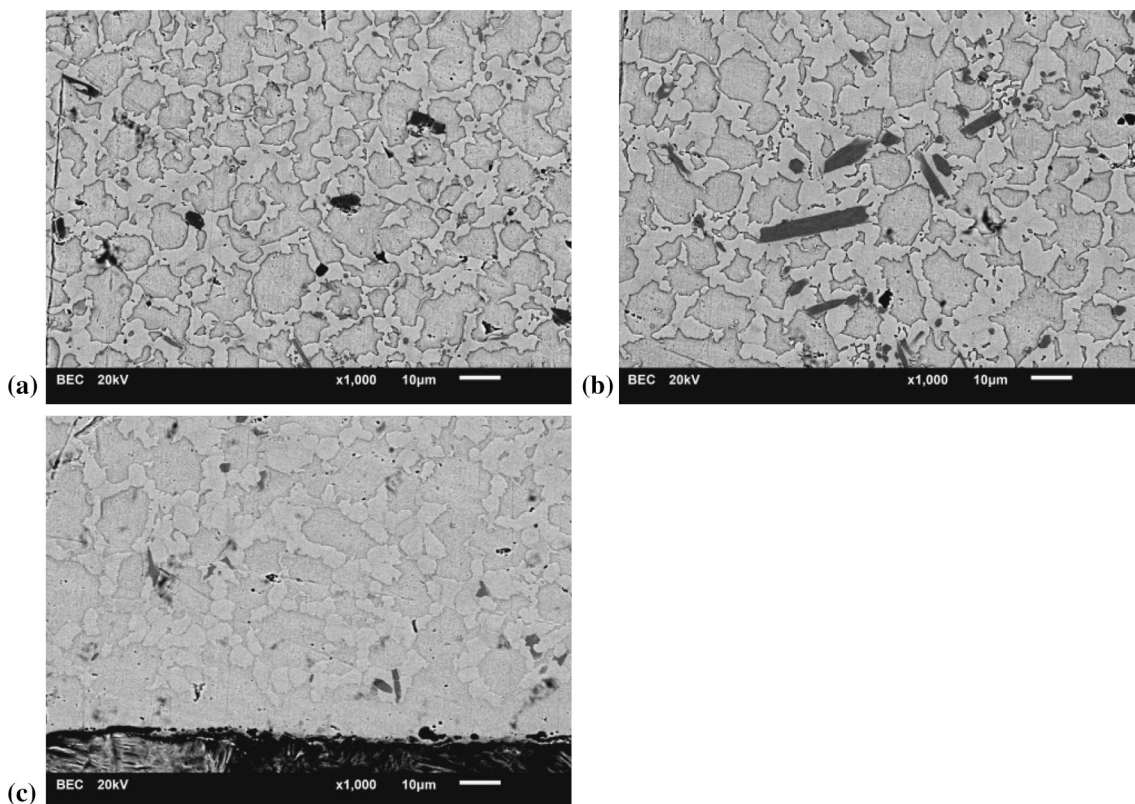


Fig. 2 Microstructure of NiCrBSi with 0% WC addition taken from: (a) top, (b) middle, and (c) bottom of coating

The scratch test was carried out nine times for each coating on the sample cross section, where the indenter started moving from the substrate surface, crossed the coating and then stopped at the mounting resin underneath as shown in Fig. 1. Cohesion was indicated by the projected area of fractured cone of coatings on the plane normal to the scratching direction. Adhesion was quantified by a crack length found in the substrate–coating interface. The higher the value, the lower the performance of cohesion, and adhesion of coating is obtained accordingly.

Additionally, the scratch tester resembles the ball on disk tribometer test, except using high load with single pass. Wear of coatings can be indirectly measured from the area of scratch track section representing the wear volume typically determined by the ball of disk method. Calculation was done on an assumption that the scratch track cross section is a segment of the circular diamond indenter tip. The larger the segment area, the more the wear is apparent.

Results and Discussion

Microstructures

Etched microstructures of NiCrBSi with 0% WC at the top, middle, and bottom sections of coating are shown in Fig. 2. There was no significant difference in the microstructures of the three sections. With the given thickness, the

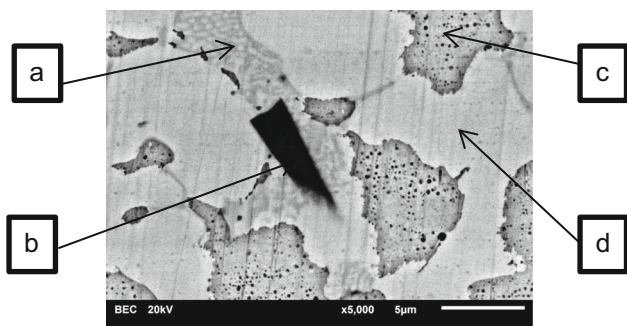


Fig. 3 Microstructure of NiCrBSi with 0% WC addition: (a) Ni₄Si; (b) Cr precipitate; (c) Ni solid solution; (d) Ni boride

Table 3 EDS results for phases in NiCrBSi with 0% WC addition

Position	Element, at.%					
	C	O	Si	Cr	Fe	Ni
Ni ₄ Si (a in Fig. 3)	14.85	2.99	15.21	2.82	1.00	63.12
Cr precipitate (b in Fig. 3)	37.50	51.76	1.26	9.48
Ni solid solution (c in Fig. 3)	16.33	2.475	7.79	6.19	2.62	64.0
Ni boride (d in Fig. 3)	13.48	...	1.16	...	2.01	83.35

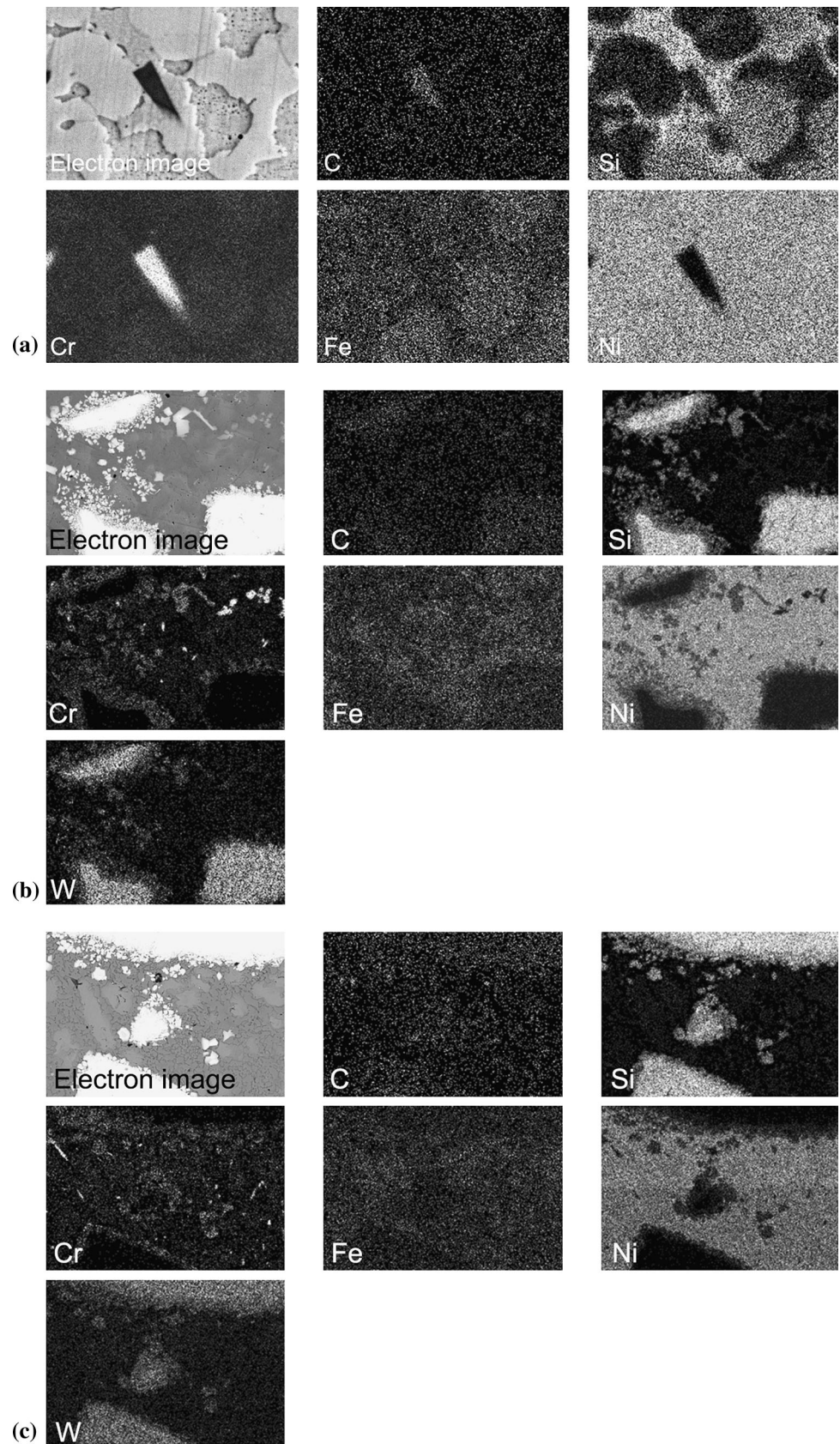
microstructures were homogeneous in which the powder was pre-alloyed before being atomized.

NiCrBSi coating shown in Fig. 3 consists of a matrix of Ni solid solution. The structure almost comprised of Ni with small amount of metallic elements, i.e., Fe and Cr, which were indicated by their solubility via phase diagram. Table 3 lists the chemical compositions of each phase examined by using EDS; the EDS results also confirmed the existence of other Ni compounds including Ni silicide. The silicide was expected to be Ni₄Si with regard to their atomic ratio and phase diagram (Ref 5). The structure was likely eutectic with Ni boride distributed in the Ni solid solution matrix. Noted that boron is a lightweight element which cannot be detected by EDS used in this study. According to Gurumoorthy et al. (Ref 7), Ni boride has a higher Cr content compared to the Ni solid solution, so that the formation of Ni boride in the coating layer can be expected and the boride should be in the form of Ni₃B as per the phase diagram (Ref 5). Cr precipitated was also distributed within the coating as black particles under the back scatter electron (BSE) image mode. A black particle shown in Fig. 3 is rich in Cr and C contents, and it is probably Cr₇C₃. All of hard phases are typically contributed to gain high wear resistance of NiCrBSi coating.

Element mappings showed in Fig. 4 indicate the distribution of chemical elements. C was found in the Cr precipitate, and Si was distributed in the Ni solid solution as well as Ni₄Si except in the Ni boride. Cr was mostly found in the Cr precipitate, and it had little amount in the Ni solid solution. Meanwhile, Ni was found abundant but not in the Cr precipitate. Little amount of Fe can be noticed in all phases particularly in the Ni solid solution.

Figure 5 shows the overall microstructure of NiCrBSi coating with 20% WC addition, and its relevant phases are noted in Fig. 6. As per the figures, the high atomic weight of WC appears as white particles in the BSE image mode. Obviously, there was no WC sinking found in the microstructure. This is due to the high melting temperature of WC that the particles cannot be fused completely into the matrix. The EDS analysis was also performed and the results are listed in Table 4, noting that W can be found in the NiCrBSi coating, especially in the Ni solid solution and Cr precipitate. The atomic weight of W at the outer area of

Fig. 4 Element mapping of NiCrBSi coating: (a) 0%; (b) 20%; (c) 40% WC addition



WC particle was found to decrease compared to the center, indicating the dissolution of W in the NiCrBSi coating.

Apparently, under the BSE image mode, the Cr precipitate was barely distinguished from other constituents, unlike the remarkable black Cr precipitate detected in the 0% WC coating (Fig. 3). The dissolution of W into the Cr precipitate makes the phase brighter due to the high molecular weight of W as shown in Fig. 7. The Ni solid solution also became brighter because of the W dissolution. Ni₄Si was difficult to be identified in this case but it plausibly located along with the Ni boride (Fig. 8).

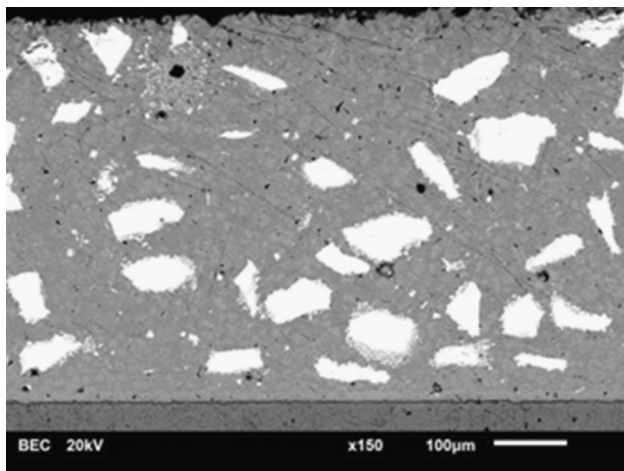


Fig. 5 Overall microstructure of NiCrBSi with 20% WC addition

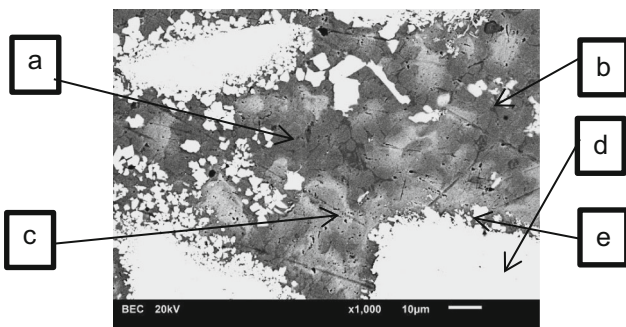


Fig. 6 Microstructure of NiCrBSi with 20% WC addition: (a) Ni₄Si and Ni boride; (b) Cr precipitate; (c) Ni solid solution; (d) WC particle; (e) diffused WC particle

Table 4 EDS results for phases in NiCrBSi with 20% WC addition

Position	Element, at. %					
	C	Si	Cr	Fe	Ni	W
WC particle (d in Fig. 6)	54.08	1.05	44.87
Diffused WC particle (e in Fig. 6)	29.22	8.41	21.05	0.58	27.05	13.70
Ni ₄ Si (a in Fig. 6)	17.35	19.40	1.54	0.86	60.85	...
Ni solid solution (c in Fig. 6)	20.12	5.44	6.27	2.77	63.56	1.83
W diffused Cr precipitate (b in Fig. 6)	48.39	...	37.87	0.46	10.58	2.69

Moreover, Cr and Ni were found to be diffused in the surface of WC particles as evidenced by a darker color around the rim of WC particles. In other words, the darker zone along the perimeter of WC particles shown in the micrographs indicates the low content of W. This could probably be happened during the fusion process when WC particles located at the outer region directly contact with melt, hence allowing Ni and Cr to diffuse into the WC particles. This phenomenon is also mentioned in Ref 16 as the outer region of WC particle is partially melted where the bonding between WC particle and NiCrBSi matrix is apparent. Such characteristics can improve the mechanical properties of coating through the solid solution strengthening. The amount of WC particle was found to be 5.90% by volume, indicating the partial dissolution of WC particle. In addition, there was no WC re-precipitated from the melted WC, as similarly reported in Ref 10, 13-15, and 17, so that the actual temperature of melt was not greater than the melting temperature of WC, even in the eutectic WC/W₂C variant. Thus, the increase in hardness is achievable accordingly.

Figure 4(b) shows the EDS maps of NiCrBSi coating with 20% WC addition. The mapping results can distinguish the Cr precipitate from the NiCrBSi background

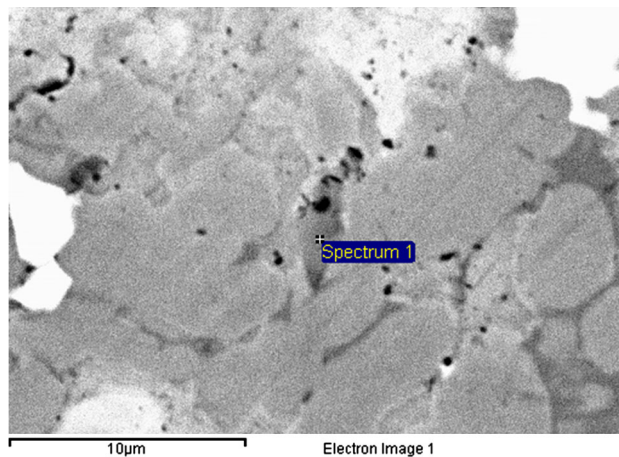


Fig. 7 W diffused into Cr precipitate in the NiCrBSi with 20% WC addition

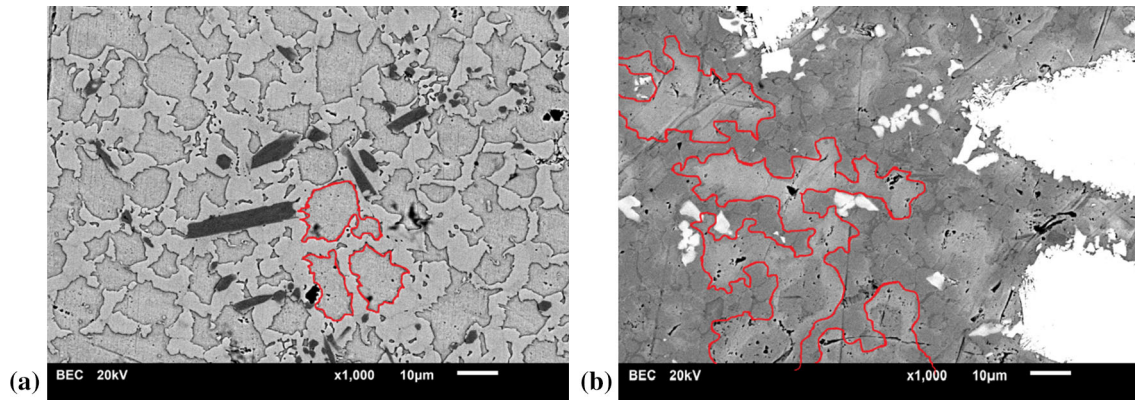


Fig. 8 Ni solid solution network of NiCrBSi: (a) 0%; (b) 20% WC addition

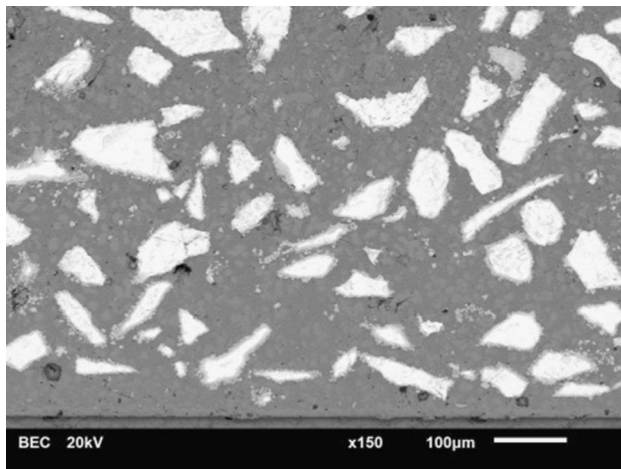


Fig. 9 Overall microstructure of NiCrBSi 40% WC coating

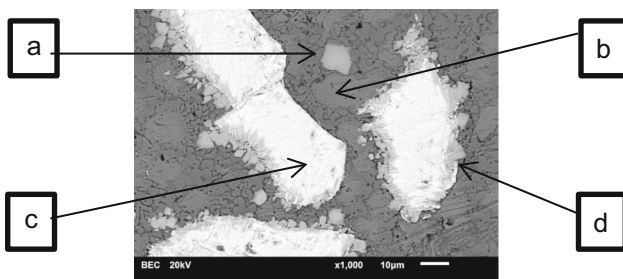


Fig. 10 Microstructure of NiCrBSi 40% WC coating: (a) Ni_4Si and Ni boride; (b) Ni solid solution; (c) WC particle; (d) diffused WC particle

matrix regarding the high amount of Cr and W. Since the W can only diffuse into the Ni solid solution, the addition of W can discern the Ni solid solution phase from the Ni boride.

By considering the coating with 40% WC addition as shown in Fig. 9 and 10, the microstructure is of similar to that of 20% WC addition, except having more remarkable dissolution of WC. In Fig. 10, the Cr precipitate is not

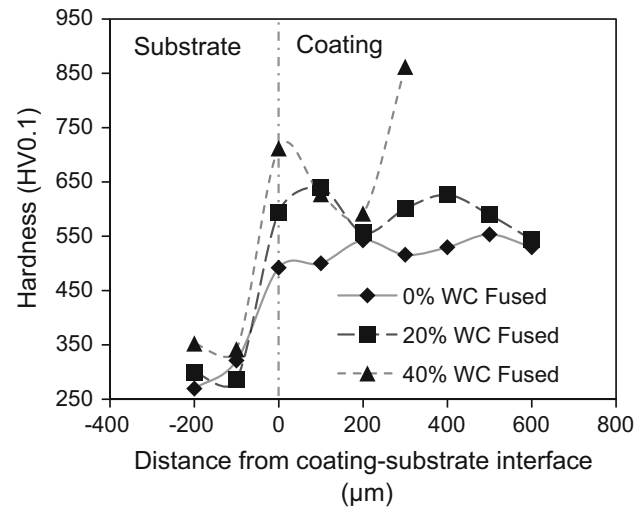


Fig. 11 Microhardness of NiCrBSi coatings

visible in the BSE image mode, but the element mapping shown in Fig. 4(c) clearly indicates the Cr precipitate location. By adding 40% WC into the coating, a greater amount of WC particles (23.29% by volume) was noticeable in the NiCrBSi coating matrix. The area of diffused WC at the outer region of particles for 40% addition was smaller than that for 20% case. This is probably due to the saturation of Ni solid solution that is reached under the large amount of WC particles, thus reducing the dissolution of WC particles.

Microhardness

Microhardness of NiCrBSi coatings reported in HV0.1 unit is plotted in Fig. 11. The average values of microhardness for substrate, 0, 20, and 40% WC addition in the NiCrBSi coating were 305, 522, 594, and 704 HV0.1, respectively. The flame spray coating obviously caused a difference in microhardness value between the coating and substrate materials. There was no microhardness gradient found in

the substrate since the substrate material was not melted during the process, thus causing no dilution and composition gradient (Ref 4, 7). The microhardness values were almost the same across the coating layer thickness. By adding WC particles into the coating, the hardness of NiCrBSi matrix was found to increase, and this is probably owing to the solid solution strengthening of W that takes place in the Ni matrix. Additionally, the W element can diffuse into the Ni solid solution matrix. This phenomenon is expected to further increase the microhardness of coating due to the W dissolution.

Cohesion and Adhesion

Cohesion and adhesion were measured by using the scratching method as described in “Experiment” Section. The micrographs of scratch track at the coating–substrate interface (adhesion) and coating–resin interface (cohesion) for 0 and 40% WC addition are presented in Fig. 12. The results revealed that under the 20 N load and 20 mm/min scratch speed, there was no crack found at the interface of coating and substrate as well as along the scratch track. This thereby indicates the good adhesion and resistance of

fracture of coatings. This characteristic is probably induced by the proper fusion process that provides a densified coating structure with less porosity, thus improving both adhesion and cohesion properties (Ref 4).

By considering at the coating–mounting resin interface, the projected area of fracture plotted in Fig. 13 was found to increase from 14,911 to 17,843 and 32,507 μm^2 for

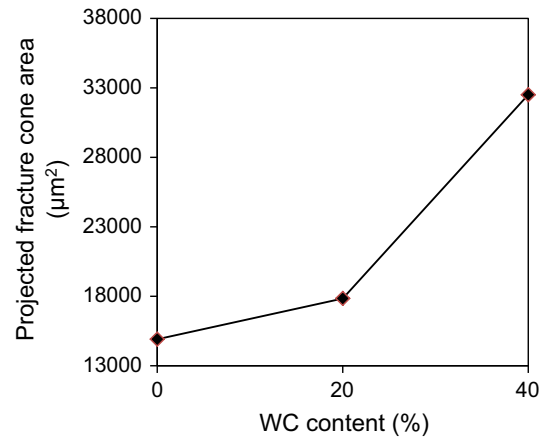


Fig. 13 Projected fracture cone area of NiCrBSi coating

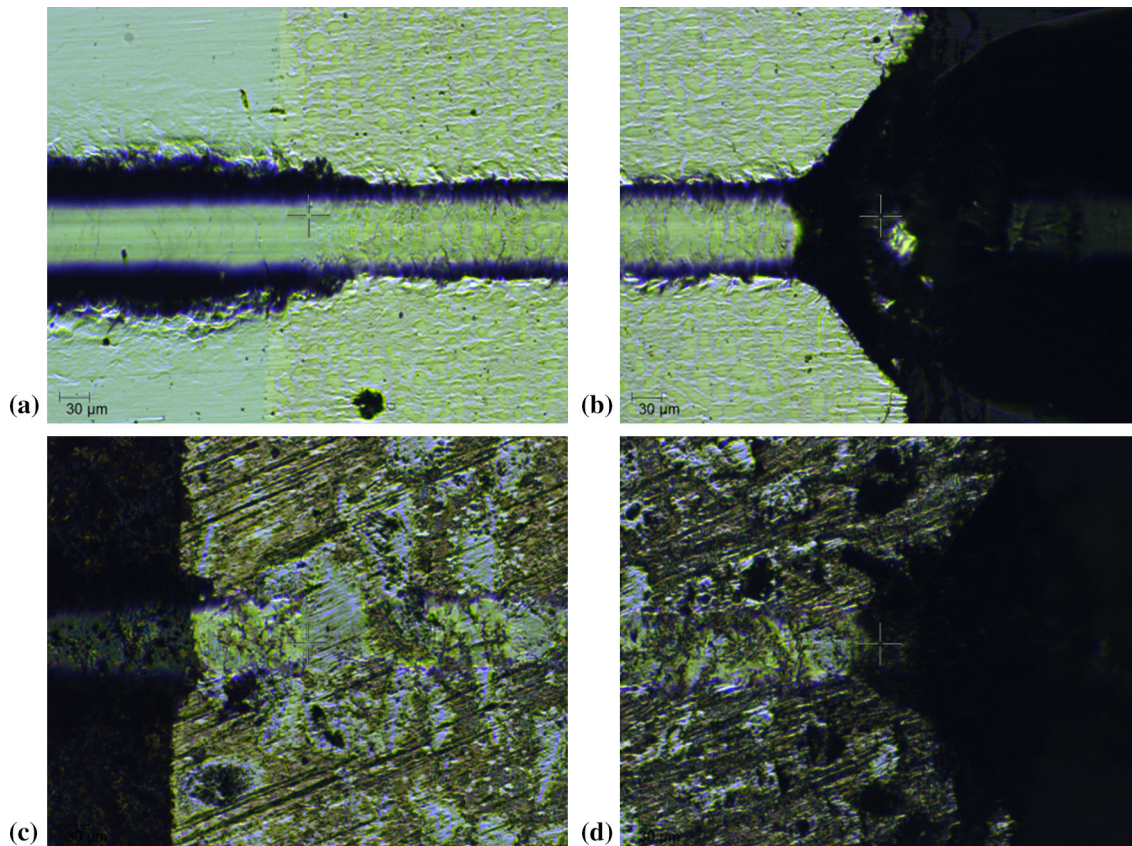


Fig. 12 Scratch track of: (a) coating–substrate interface; (b) coating–resin interface of NiCrBSi 0% WC; (c) coating–substrate interface; (d) coating–resin interface of NiCrBSi 40% WC

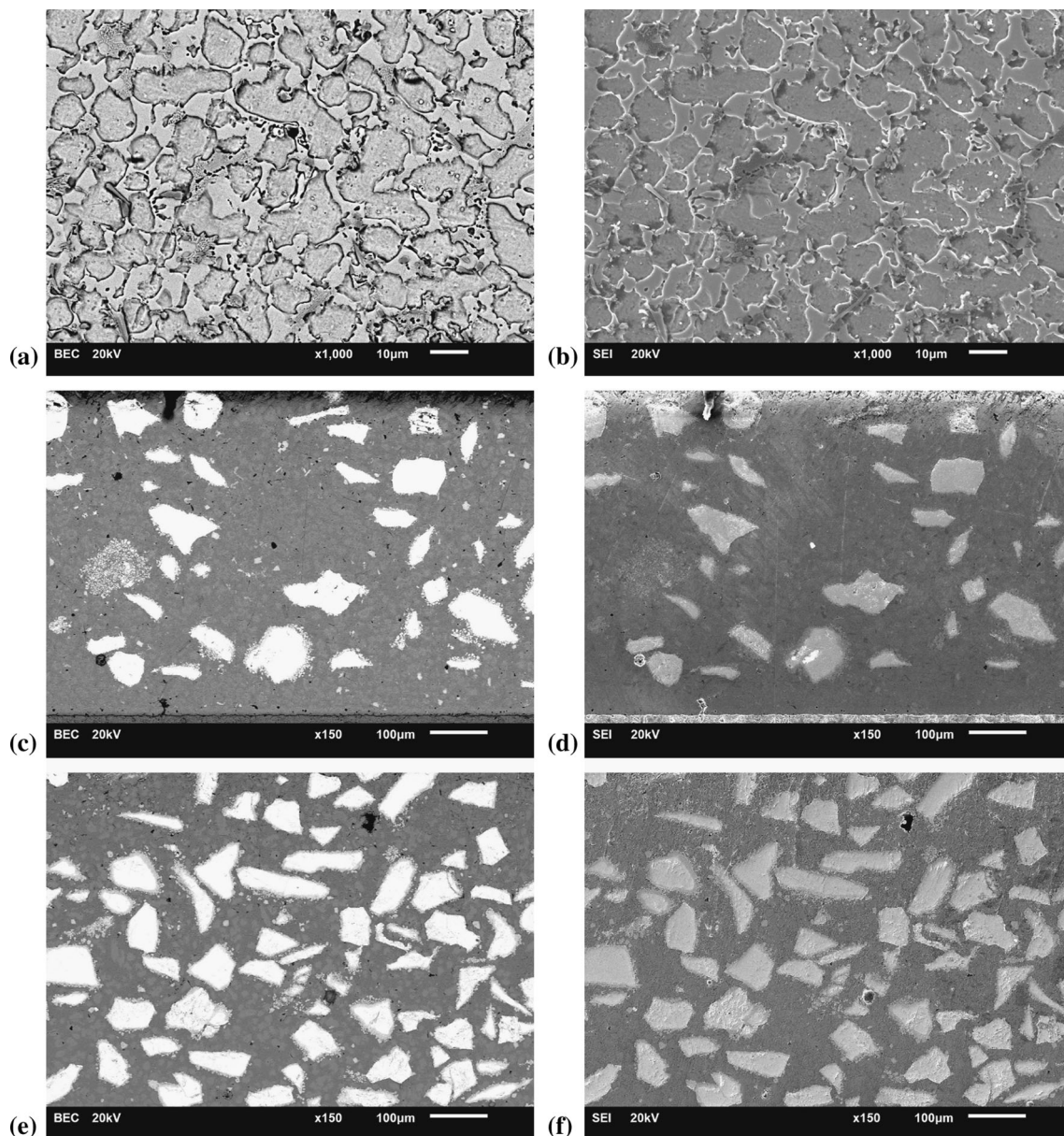


Fig. 14 Microstructure of NiCrBSi coating with: (a) 0% WC (BSE); (b) 0% WC (SEI); (c) 20% WC (BSE); (d) 20% WC (SEI); (e) 40% WC (BSE); (f) 40% WC (SEI)

coating with 0, 20, and 40% WC addition, respectively. The reduction in cohesion performance is probably originated from the W dissolution that substantially promotes brittleness and increases porosity in the coating matrix with the addition of WC as shown in Fig. 14. The amount of porosity found in the coating with 0, 20, and 40% WC addition was 0.22, 0.83, and 1.27%, respectively.

Rigidity of Coatings

Based on the scratch test, the rigidity of coatings was quantified from the cross-section area of scratch track. The

cross-section area of scratch track for all coatings was significantly smaller than the substrate because of higher hardness as shown in Fig. 15. Furthermore, the NiCrBSi coatings with 0, 20, and 40% WC addition can improve the average rigidity by 437, 484, and 746% compared to the substrate material. The reinforcement of WC and solid solution strengthening of W in Ni are responsible for this improvement. With regard to the linear relationship between relative hardness and rigidity plotted in Fig. 16, the graph slope is approximately 5. This can be implied that when the hardness is increased by 100%, the wear resistance could be improved by 500% approximately.

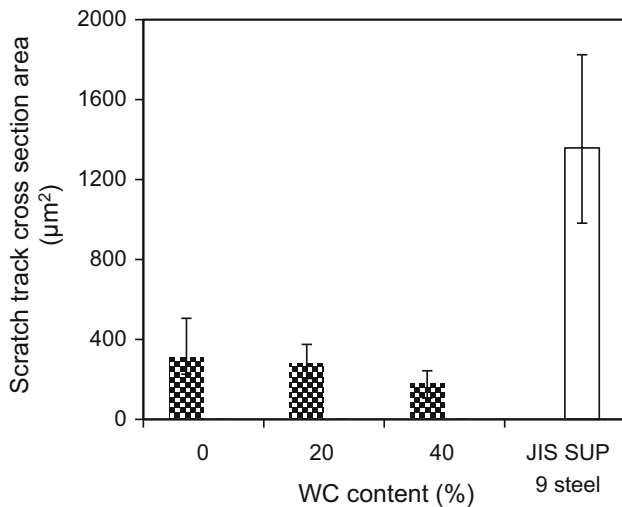


Fig. 15 Scratch track cross-section area of NiCrBSi coating

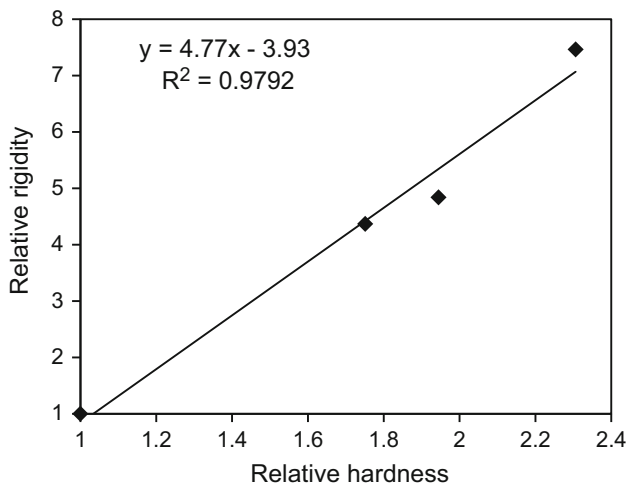


Fig. 16 Relationship between relative hardness and rigidity

Conclusions

The dissolution of WC particle was expected to create free W that later diffused into the NiCrBSi matrix particularly in the Ni solid solution and Cr precipitate. In addition, the re-solidifying of carbide was not apparent in the coating due to the low heat input. The hardness of coating was found to increase with the amount of WC addition. However, the presence of WC in the coating deteriorated the cohesion property due to the brittleness. Based on the microstructure analyses, there was no sign of WC melting as well as WC sinking at the bottom of coating layer.

Acknowledgments This work is a part of “Application of Thermal Spray in Agricultural Part” project, supported by Innovation and Technology Assistance Program (iTAP) under National Science and Technology Development Agency (NSTDA) and Acme International (Thailand) Ltd. The authors would like to express their gratitude and gratefully acknowledge.

References

- M.A. Garrido, A. Rico, M.T. Gómez, M. Cadenas, J.E. Fernández-Rico, and J. Rodríguez, Tribological and Oxidative Behavior of Thermally Sprayed NiCrBSi Coatings, *J. Therm. Spray Technol.*, 2017, **26**, p 517-529
- K. Bobzin, M. Öte, T.F. Linke, and K.M. Malik, Wear and Corrosion Resistance of Fe-Based Coatings Reinforced by TiC Particles for Application in Hydraulic Systems, *J. Therm. Spray Technol.*, 2016, **25**, p 365-374
- R. González, M. Cadenas, R. Fernández, J.L. Cortizo, and E. Rodríguez, Wear Behaviour of Flame Sprayed NiCrBSi Coating Remelted by Flame or by Laser, *Wear*, 2007, **262**, p 301-307
- J.R. Davis, *Handbook of Thermal Spray Technology*, ASM International, Almere, 2004
- J.R. Davis, *ASM Specialty Handbook: Nickel, Cobalt, and Their Alloys*, ASM International, Almere, 2000
- C. Navas, R. Colaço, J. de Damborenea, and R. Vilar, Abrasive Wear Behaviour of Laser Clad and Flame Sprayed-Melted NiCrBSi Coatings, *Surf. Coat. Technol.*, 2006, **200**, p 6854-6862
- K. Gurumoorthy, M. Kamaraj, K.P. Rao, A.S. Rao, and S. Venugopal, Microstructural Aspects of Plasma Transferred Arc Surfaced Ni-Based Hardfacing Alloy, *Mater. Sci. Eng. A*, 2007, **456**, p 11-19
- S. Dong, B. Song, H. Liao, and C. Coddet, Deposition of NiCrBSi Coatings by Atmospheric Plasma Spraying and Dry-Ice Blasting: Microstructure and Wear Resistance, *Surf. Coat. Technol.*, 2015, **268**, p 36-45
- A. Vencl, S. Arostegui, G. Favaro, F. Zivic, M. Mrdak, S. Mitrovic, and V. Popovic, Evaluation of Adhesion/Cohesion Bond Strength of the thick Plasma Spray Coatings by Scratch Testing on Coatings Cross-Sections, *Tribol. Int.*, 2011, **44**, p 1281-1288
- P. Niranatlumpong and H. Koiprasert, Phase Transformation of NiCrBSi-WC and NiBSi-WC Arc Sprayed Coatings, *Surf. Coat. Technol.*, 2011, **206**, p 440-445
- H. Yu, W. Zhang, H. Wang, Y. Guo, M. Wei, Z. Song, and Y. Wang, Bonding and Sliding Wear Behaviors of the Plasma Sprayed NiCrBSi Coatings, *Tribol. Int.*, 2013, **66**, p 105-113
- P. Reinaldo and A.S. D’Oliveira, NiCrSiB Coatings Deposited by Plasma Transferred Arc on Different Steel Substrates, *J. Mater. Eng. Perform.*, 2011, **22**, p 590-597
- S.W. Huang, M. Samandi, and M. Brandt, Abrasive Wear Performance and Microstructure of Laser Clad WC/Ni Layers, *Wear*, 2004, **256**, p 1095-1105
- M.R. Fernández, A. García, J.M. Cuetos, R. González, A. Noriega, and M. Cadenas, Effect of Actual WC Content on the Reciprocating Wear of a Laser Cladding NiCrBSi Alloy Reinforced with WC, *Wear*, 2015, **324-325**, p 80-89
- K. Van Acker, D. Vanhoyweghen, R. Persoons, and J. Vangrunderbeek, Influence of Tungsten Carbide Particle Size and Distribution on the Wear Resistance of Laser Clad WC/Ni Coatings, *Wear*, 2005, **258**, p 194-202
- M.J. Tobar, C. Álvarez, J.M. Amado, G. Rodríguez, and A. Yáñez, Morphology and Characterization of Laser Clad Composite NiCrBSi-WC Coatings on Stainless Steel, *Surf. Coat. Technol.*, 2006, **200**, p 6313-6317

17. P.F. Mendez, N. Barnes, K. Bell, S.D. Borle, S.S. Gajapathi, S.D. Guest, H. Izadi, A.K. Gol, and G. Wood, Welding Processes for Wear Resistant Overlays, *J. Manuf. Process.*, 2014, **16**, p 4-25
18. D. Deschuyteneer, F. Petit, M. Gonon, and F. Cambier, Processing and Characterization of Laser Clad NiCrBSi/WC Composite Coatings—Influence of Microstructure on Hardness and Wear, *Surf. Coat. Technol.*, 2015, **283**, p 162-171

Publisher's Note Springer Nature remains neutral with regard to jurisdictional claims in published maps and institutional affiliations.